Journal of Materials and Electronic Devices 2 (2025) 78-82

JOURNAL OF MATERIALS AND ELECTRONIC DEVICES
JMED

Ag substitution effect on $NdBa_2Cu_3O_z$ high- T_c superconductor system

Mehmet Eyyüphan YAKINCI*

Iskenderun Technical University, Faculty of Engineering and Natural Sciences, Department of Metallurgy and Materials Engineering, 31200-Iskenderun, Hatay-Türkiye

Many research teams are actively studying $NdBa_2Cu_3O_x$-based High-T_c superconducting systems, conducting experimental and theoretical research to adapt them for technological use and enable various applications. The fact that these materials have a high transition temperature of 94 K and maintain good current-carrying capacity even under strong magnetic fields makes them a preferred choice for many uses. This study examines how 1% Ag substitution affects the overall properties of the $NdBa_2Cu_3O_x$ superconducting system. The results show that Ag substitution did not significantly change the crystal structure of the base material. However, the superconducting transition temperature increased by 1.5 K, and the critical current density reached 4.9 x 10^5 A/cm². Additionally, no impurities were detected in the structure due to Ag substitution, which also showed stabilizing effects concerning O_2 concentration. This is believed to further enhance the usability of $Nd_{0.9}Ag_{0.1}Ba_2Cu_3Ox$ in high-tech applications.

Keywords: *High Tc superconductors, $NdBa_2O_{7+z}$ superconductors, Ag substituted NdBaCuO superconductors*

Submission Date: 26 September 2025
Acceptance Date: 06 December 2025

**Corresponding author: meyyuphan.yakinci@iste.edu.tr*

1. Introduction

Although most properties of $ReBa_2Cu_3O_x$ high-temperature superconductors, discovered in the late 1980s, are well known, significant research is still ongoing to discover new properties or to improve superconducting performance compared to current capabilities [1-3]. These studies mainly focus on increasing the critical current density (J_c) and superconducting transition temperature (T_c) beyond their existing levels, along with theoretical research to guide these efforts. This is essential because, for high-tech applications today, these materials must meet high standards in electrical conductivity. At a minimum, a T_c value significantly above 77 K and a J_c around 5 K, with a current density close to 10^6 A/cm², are expected. NdBaCuO-based superconductors are a well-known superconducting material that meets these conditions but has room for improvement, and significant research is ongoing in this area.

Compared to YBaCuO, which holds an important position within the ReBaCuO family, it offers a few kelvin higher critical transition temperature, much better pinning ability, greater critical current capacity, and roughly 10 times lower oxygen partial pressure, making this material more advantageous among ReBaCuO superconductors [2-8]. Due to these properties, NdBaCuO-based superconductors have the potential to be used in scientific studies in spintronics and related theoretical research, small fusion reactors, fault current limiters, and in the development of new devices such as magnetic imaging systems for medical applications, which are critical components in healthcare [9,10].

However, it is known that there are some important problems to consider during the preparation of NdBaCuO-based superconductors. Especially when annealing in an O_2 atmosphere, the O_2 gas pressure is quite critical. When processing occurs in a high oxygen environment, the formation of impurity phases and reduced superconducting performance are inevitable [8-15]. However, when the pressure is kept low and a slow cooling process is used, the superconducting performance significantly improves,

making it possible to achieve a single-phase structure. Furthermore, adding a small amount of flux material to the structure can greatly enhance crystal formation. Ultimately, this can directly improve superconducting performance. In this study, instead of Nd 1% Ag as a flux material, a nominal composition of $Nd_{0.9}Ag_{0.1}Ba_2Cu_3O_x$ was produced using the solid-state method, and its structural, electrical and magnetic properties including critical current density were investigated and the results obtained are presented.

2. Experimental

In this study, $Nd_{0.9}Ag_{0.1}Ba_2Cu_3O_x$ material was produced with a single-phase structure using the solid-state method. The samples prepared used high-purity raw materials of Y2O3 99.99% (Sigma-Aldrich), AgO 99.9% (Sigma-Aldrich), BaCO3 99.99% (Sigma-Aldrich), CuO 99.99% (Sigma-Aldrich), and MgO 99.99% (Sigma-Aldrich). The raw powders, combined in appropriate ratios, were mixed in an agate mortar for 2 hours. The first calcination was performed in a platinum crucible at 870°C for 20 hours, then the furnace was naturally cooled. The material removed from the furnace was ground again in an agate mortar, and the same calcination process was repeated. Next, the pelletizing process began, with the finely powdered material pressed into pellets under 7 tons of pressure, each with a diameter of 10 mm. Two grams of calcined powder were used for each pellet. The pellets were then heated to 1035°C at a slow rate of 1°C/min, held at this temperature for 60 minutes, cooled to 935°C at 1°C/min, and maintained for 75 minutes. During this heating, the samples received a gas mixture of 2% O_2 + 98% Ar from the start. Afterward, the samples cooled to 475°C at 5°C/min and were kept in a pure O_2 environment for 60 hours. Finally, the furnace was turned off and allowed to cool to room temperature.

The initial analysis of the samples prepared in this format was conducted using X-ray diffraction (XRD). For this purpose, the Malvern-Panalytical Empyrean system and CuK_α radiation between 2θ = 3-80° were utilized. After verifying the results with the Rietveld method, the crystal parameters were calculated using the least-squares fitting method. For electrical and magnetic measurements, the Quantum Design Physical Property Measurement System, PPMS-9T, with Vibrating Sample Magnetometer (VSM) attachment, operated under a magnetic field of ± 8 T for PPMS and ± 9 T for VSM system, was employed. *I-V* characterizations of the samples at 5, 20 and 40 K were also performed within the PPMS system under zero-field conditions.

3. Results and Discussions

The XRD patterns of the prepared samples are shown in Fig. 1. As depicted in Fig. 1, the Ag-substituted sample displays no impurity phase related to Ag or other impurities and exhibits sharp peaks. Four different pellets in the same batch were analyzed, and all showed the same crystal structure. Therefore, it was concluded that the samples were produced as single-phase. The calculated crystal structure parameters are a=3.8617 Å, b=3.9164 Å, c=11.7693 Å. The unit cell volume was found to be 178.001 Å³. Additionally, calculations indicated that the crystal system is orthorhombic. This aligns with previous calculations for $Nd_{0.9}Ag_{0.1}Ba_2Cu_3O_x$ material, showing minor variation attributable to Ag substitution.

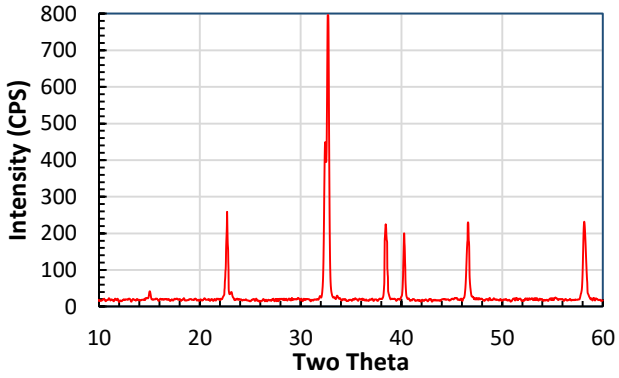

Fig.1. XRD graphs of the $Nd_{0.9}Ag_{0.1}Ba_2Cu_3O_x$ single-phase sample.

The electrical resistance measurements of the produced samples between magnetic fields of zero and 8 Tesla are shown in Fig. 2. Our investigations involved taking repeated measurements on 4 different pellets from the samples, and all samples exhibited metallic behavior from room temperature up to the T_c value. Then, they transitioned sharply to the superconducting, T_{zero}, state. Meanwhile, the 4 different samples measured displayed the same electrical behavior and superconducting performance. Due to the Ag substitution, no anomalies caused by secondary or impurity phases were observed. Accordingly, all samples began to undergo a phase change at 97 K under zero magnetic field and became superconducting at 95 K.

However, with an applied field, both T_c and T_{zero} values decreased significantly, showing the typical behavior of Type II superconductors, Fig. 2. Nonetheless, the fact that the samples maintained superconducting behavior even under an 8 T field indicates that this material could be used in technological applications. The results measured under zero field were approximately 1.5 K higher than those of undoped $NdBa_2Cu_3O_x$ samples. This is likely due to the prevention of different phases forming within the sample

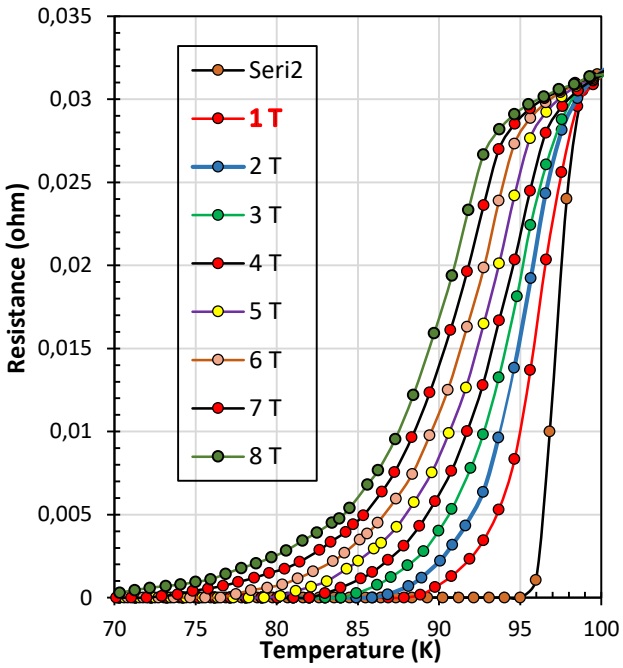

Fig.2. *MR-T* measurements of $Nd_{0.9}Ag_{0.1}Ba_2Cu_3O_x$ superconductor sample under 8 T magnetic field.

and/or the reduction of agglomerations or dislocations at the atomic level, resulting in clearer conductivity in the structure. In other words, this likely reduces scattering and enhances superconductivity. Magnetic measurements of the prepared samples were performed using a VSM system up to 9 Tesla at temperatures of 5, 20, and 40 K. The results follow the *M-H* curves typical of classical Type II superconductors and show properties consistent with $ReBa_2Cu_3O_x$ High-T_c superconductors, Fig. 3. No phase or state indicating a change in magnetic properties across the tested temperatures was observed; in other words, there was no deviation from diamagnetism in the curves.

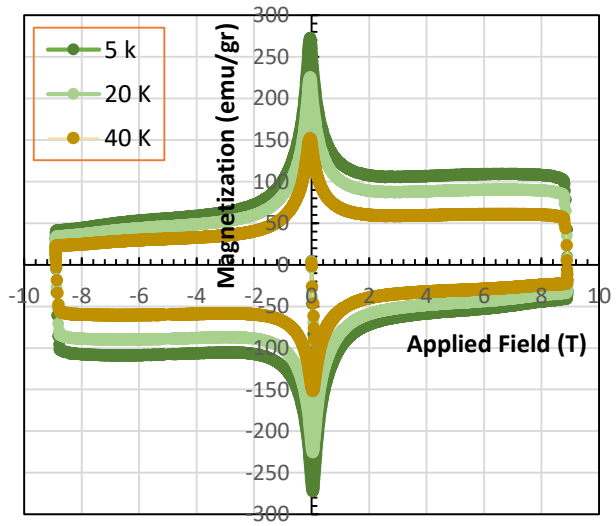

Fig.3. Magnetization versus applied field (*M-H*) measurement of the sample prepared.

However, as expected for Type II High-T_c materials, a significant decrease in magnetization with increasing temperature was noted. Interestingly, the reduction in magnetization with temperature was less than expected, which clearly highlights the purity and quality of the samples produced. The magnetization value of ± 270 emu/g at 5 K provides strong supporting evidence. This clearly shows that the samples produced, with magnetization values of ± 240 emu/g at 20 K and ± 155 emu/g at 40 K, and displaying no deviation from diamagnetism (such as ferromagnetism), are single-phase and suitable for technological applications. It also demonstrates that Ag substitution positively affects $NdBa_2Cu_3O_x$-based superconducting materials by encouraging the formation of a single-phase material. measurements of the superconducting samples.

The critical current densities of the samples were measured using two different methods. First, four consecutive *I-V* measurements were taken on 5 x 10 x 2 mm samples cut at constant temperatures of 5, 20, and 40 K under zero field in the PPMS system. All measured samples produced similar results, with a variation of ± 1%. The best values are plotted in Fig. 4, and all results are listed in Table 1. The measurements were also evaluated using the 1 µV criterion, which is the international standard for *I-V* analyses. Accordingly, the best result was obtained at 5 K, with a value of J_c = 1936 A/cm².

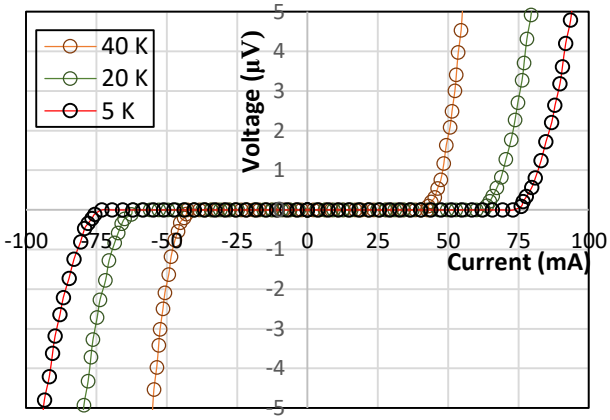

Fig.4. *I-V* measurement results at 5, 20 and 40 K and at zero applied field.

Secondly, by analyzing the *M-H* curves, the critical current density, J_c^{mag}, as a function of the magnetic field, was calculated using the Bean current density model.

Table 2. Critical Current Density, J_c and J_c^{mag} values of the samples at zero field.

Measurement Temperature, (K)	J_c (A/cm²)	J_c^{mag} (A/cm²)
5	1936	$4.9x10^5$
20	1718	$1.2x10^5$
40	1377	$8,9x10^4$

Accordingly, the Bean model is expressed as follows [2,11];

$$J_c^{mag} = 20\frac{\Delta M}{a(1-\frac{a}{3b})} \quad (1)$$

In this formula, a and b represent the lengths of the sample cross-section in centimeters (with a < b), and ΔM is the difference between the magnetization measured during decreasing and increasing the applied field in ± emu·cm⁻³. The graphs of measurements taken at temperatures of 5, 20, and 40 K, with magnetic fields up to 9 T, are shown in Fig. 5.

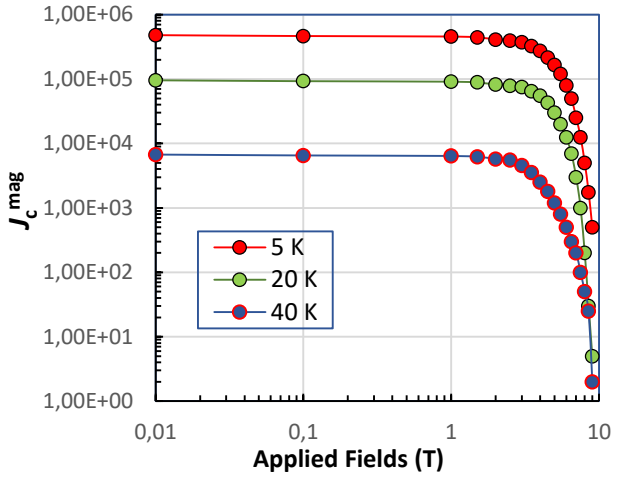

Fig.5. J_c^{mag} calculations result of the sample at different applied fields.

Accordingly, the best result was obtained from the sample measured at 5 K under zero field, with a value of 4.9 x 10^5 A/cm². In the same sample, superconductivity persisted even under a 9 T field, with a J_c^{mag} value of 6.0 x 10^3 A/cm². For the sample measured at 20 K, the J_c^{mag} value was 1.2 x 10^5 A/cm² under zero field and about 200 A/cm² at 9 T. At 40 K, the measured values were 8.9 x 10^4 A/cm² in zero field and 92 A/cm² at 9 T. However, these values clearly decrease as the measurement temperature increases, due to the nature of Type II superconductors, Fig. 5.

Upon examination, it is clear that there are two distinct slopes at low temperatures at 5 K and three distinct slopes at 20 and 40 K. On these slopes, the slope increases, especially at high $\mu_0 H$ values. This indicates that, according to the power law $J \sim H^{-\alpha}$, the α- value is approximately 0.20 between 0.1 and 4 T, and the samples exhibit weak sensitivity to the applied magnetic field. However, as the field strength increases, the α- value also rises and approaches about 0.6. This demonstrates that a strong pinning mechanism has begun all over the samples.

However, after 4.5 Tesla applied field, the increase in the slope and consequently the α- value approaches 1, which is interpreted as the pinning centers being covered by vortices, as described in previously made similar studies in different superconducting materials [12-15]. In general, it can be summarized that the strong pinning mechanism become dominant at low temperatures but at high applied fields or at high temperatures other than 5 K vortex motion become dominant and pinning centers were covered by the vortexes on the surface of the samples.

4. Conclusions

In this study, superconducting materials with a nominal composition of $Nd_{0.9}Ag_{0.1}Ba_2Cu_3O_x$ were prepared by substituting AgO into an NdBaCuO superconducting base system. A slightly different heat treatment than that described in the existing literature was carefully applied, and single-phase superconducting samples were produced. The effect of Ag doping on the NdBaCuO superconducting system was investigated by means of electrical and magnetic peculiarities. The results showed that Ag helped produce a single-phase material without causing any agglomeration in the NdBaCuO system and exhibited a stabilizing property, especially regarding oxygen concentration.

It was also observed that it prevented the formation of potential interphases while maintaining metallic properties in terms of electrical conductivity. The fact that the produced samples strongly exhibited classical Type II properties showed that this material can be used in many high technology equipment productions such as MR or high field magnet applications. The obtained critical current density values also showed improvement compared to the undoped $NdBa_2Cu_3O_x$ superconducting system. This demonstrates the positive effect of Ag substitution. It has been assessed that this High-T_c material can be easily produced not only in bulk but also in wire, strip, and thin/thick film forms, and that it can be used in high-technology applications further.

References

[1] Cicek, O. and Yakinci, K., Structural, Magneto-Resistivity and Magnetization Investigations of Y(Ba1−xMgx)2Cu3O7−δ Superconducting System, Acta Physica Polonica A, 2022. 4, 142.

[2] Cicek, O. and Yakinci, K. Enhanced superconducting properties of multi-wall carbon nanotubes added YBCO-123 Superconducting System, Journal of Molecular Structure, 2020. 1211, 128089.

[3] I. Monot a, F. Tancret, P. Laffez, G. Van Tendeloo, G. Desgardin, Microstructure and properties of oxygen controlled melt textured NdBaCuO superconductive ceramics, Materials Science and Engineering B65 (1999) 26–34.

[4] W. Bieger, G. C-abbes, P. Schgtzle, A. Leistikocv, J. Thomas, P. Verges, microstructure and improved properties of NdBaCuO bulk materials, Materials Science and Engineering B53 (1998) 100-103.

[5] E. H. Sujionoa, A. H. Khatimaha, A. N. Hasanaha, N. F. Mahendia, M. Y. Dahlana, N. A. Humairaha, A. Irhamsyaha, Nd(Fe)0.3Ba1.7Cu3O7-δ Oxide Material Crystal Structure and Morphological Analysis, Materials Today: Proceedings, 13 (2019) 264–269.

[6] Sujionoa, E. H., Khatimaha, A. H., Hasanaha, A. N., Mahendia, N. F., Dahlana, M. Y., Humairaha, N. A., Irhamsyaha, A., Nd(Fe)0.3Ba1.7Cu3O7-δ Oxide Material Crystal Structure and Morphological Analysis, Materials Today: Proceedings, 2019. 13, 264–269.

[7] F. Tancret, I. Monot, P. Laffez, G. Van Tendeloo, G. Desgardin. Preparation and characterization of melt textured $NdBa_2Cu_3O_{7-\delta}$ bulk superconducting ceramics, Phys. J-Appl. Phys. 1(1998)185-190.

[8] Huang, R.T., Chen, J., Liu, Z.Y., Wang, G., Cai, C.B.: Significantly improving the flux pinning of $YBa_2Cu_3O_7$-δ superconducting coated conductors via $BaHfO_3$ nanocrystal addition using multistep film growth method. Adv. Funct. Mater, 2024. 24, 01251.

[9] Okada, T., Gaifullin, M., Vyatkin, V., Dao, H.T., Veshchunov, I., Petrykin, V., Lee, S., Awaji, S.A.: Reduction of Jc anisotropy in REBCO coated conductors via bilayer structure of columnar and random pinning centers. Supercond. Sci. Technol., 2025. 38, 055021.

[10] Abdelhaleem, S., Alruwaili, A., Alziyadi, M.O., Yakinci, K. and Shalaby, M.S., Anomalous magnetization reversal and superconducting $Bi_2Sr_2Ca_{1-x}V_yGd_xCu_2O_{8\pm\delta}$ nanocomposites. J Mater Sci: Mater Electron, 2025. 36, 1433.

[11] Yakinci, K. and Cicek, O., Role of Multi-Walled Carbon Nanotube Addition in Superconducting Properties of Bi2Sr2CaCu2O8+sGlass–Ceramic Superconductors, Acta Physica Polonica A, 2023. 4, 143.

[12] Li, Z.G., Wei, S.Q., Zhang, J.L., Bu, Y.H., Wang, D.H., Xiao, G.Y., Jin, H., Qin, J.G., Zhou, C., Zhang, Z., Current-carrying and mechanical properties of REBCO multi-filamentary tapes after electroplated copper re-encapsulation. Supercond. Sci. Technol., 2025. 38, 045015.

[13] Zhang, Y.X., Li, W.H., Yong, L.W., Peng, S.S., Zhou, D.F., Zhang, Y.B., Yin, X.M., Cai, C.B., Design and test of HTS rotor magnets for high energy density motor. Supercond. Sci. Technol., 2025. 38, 055020.

[14] Huang, R.T., Chen, J., Liu, Z.Y., Dou, W.Z., Zhang, N., Cai, C.B., Monodisperse BaZrO3 nanocrystals and flux pinning effect on upscaling MOD-derived (Y,Dy)Ba2Cu3O7−δ superconducting tapes. Supercond. Sci. Technol., 2023. 36, 125002

[15] Dong, C.H., Lin, H., Huang, H., Yao, C., Zhang, X.P., Wang, D.L., Zhang, Q.J., Ma, Y.W., Awaji, S., Watanabe, K., Vortex pinning and dynamics in high performance Sr0.6K0.4Fe2As2 superconductor, J Appl. Phys. 2016. 119, 143906